Neuronal replacement from endogenous precursors in the adult brain after stroke.

Arvidsson, Andreas; Collin, Tove; Kirik, Deniz; Kokaia, Zaal; Lindvall, Olle

Published in:
Nature Medicine

DOI:
10.1038/nm747

2002

Neuronal replacement from endogenous precursors in the adult brain after stroke

ANDREAS ARVIDSSON[1], TOVE COLLIN[1], DENIZ KIRIK[2], ZAAL KOKAIA[1] & OLLE LINDVALL[1]

[1]*Section of Restorative Neurology and* [2]*Neurobiology, Wallenberg Neuroscience Center, Lund University Hospital, Lund, Sweden*
Correspondence should be addressed to A.A.; email: andreas.arvidsson@neurol.lu.se
Z.K. and O.L. contributed equally to this study.

Published online: 5 August 2002, corrected online 30 August 2002 (details online); doi:10.1038/nm747

In the adult brain, new neurons are continuously generated in the subventricular zone and dentate gyrus, but it is unknown whether these neurons can replace those lost following damage or disease. Here we show that stroke, caused by transient middle cerebral artery occlusion in adult rats, leads to a marked increase of cell proliferation in the subventricular zone. Stroke-generated new neurons, as well as neuroblasts probably already formed before the insult, migrate into the severely damaged area of the striatum, where they express markers of developing and mature, striatal medium-sized spiny neurons. Thus, stroke induces differentiation of new neurons into the phenotype of most of the neurons destroyed by the ischemic lesion. Here we show that the adult brain has the capacity for self-repair after insults causing extensive neuronal death. If the new neurons are functional and their formation can be stimulated, a novel therapeutic strategy might be developed for stroke in humans.

The generation of new neurons in the adult brain is largely restricted to two regions: the subventricular zone (SVZ) lining the lateral ventricles, and the subgranular zone (SGZ) of the dentate gyrus (DG)[1]. Additional neuronal progenitors reside in the forebrain parenchyma[2]. Brain insults such as cerebral ischemia and epileptic seizures, which cause neuronal death, are accompanied by increased neurogenesis in the SGZ (refs. 3–6) and SVZ (refs. 7,8), whereas it is unclear if new neurons are formed in other regions[8,9].

From the clinical perspective, a fundamental question is whether the new neurons can migrate to the site of injury and replace neurons that have died. The evidence for such neuronal self-repair in the adult brain is scarce. Magavi *et al.*[10] used targeted apoptosis of cortical pyramidal neurons and found a small number of new neurons extending processes to the original target sites in the thalamus. However, this lesion destroyed only the targeted neurons without affecting the surrounding tissue. Whether neuronal replacement from endogenous precursors occurs following extensive lesions resembling human disease is unknown.

Here we investigated whether new neurons are formed in the adult rat striatum after stroke induced by two hours of middle cerebral artery occlusion (MCAO). This ischemic insult causes infarction in the striatum and parietal cortex. We show that stroke leads to increased neurogenesis in the SVZ. New neurons migrate into the damaged striatal area, where they express morphological markers characteristic of most of the dead neurons, that is, medium-sized spiny neurons[11]. In the intact brain, these neurons project to the globus pallidus and substantia nigra and form part of the basal ganglia motor circuitry.

Stroke leads to neurogenesis in damaged striatum

At five weeks after stroke, there was an almost complete loss of cells immunoreactive for the neuron-specific marker NeuN in the lateral and caudal parts of the ipsilateral striatum, whereas the most medial and frontal parts were often spared. To label dividing cells we used 5-bromo-2′-deoxyuridine (BrdU), a thymidine analog that is incorporated into DNA during cell division. BrdU was injected twice daily during days 4–6 after stroke or sham procedure. At 4 weeks after the last injection, few BrdU-NeuN double-labeled, presumably newly formed neurons were observed in the striatum ipsilateral to sham surgery. Stroke gave rise to a 31-fold increase of the number of BrdU-NeuN-labeled neurons in the ipsilateral striatum (Fig. 1*a*) (n = 9 and 10 for MCAO and sham, respectively; $P < 0.005$, Mann–Whitney U-test), whereas the number in the contralateral striatum was similar to that in control (data not shown). There were numerous BrdU-labeled cells not expressing NeuN in the ischemic brain tissue, reflecting massive gliosis and inflammatory reaction[12,13]. Parts of the damaged striatal tissue had often disintegrated and were not available for analysis. Therefore, the stroke-induced increase of BrdU-NeuN double-labeled cells was even more pronounced when cell densities were compared between ischemic and sham-operated animals (136.7 ± 66.7 and 0.8 ± 0.3 cells per mm^3, respectively; $P < 0.0005$, Mann–Whitney U-test) (Fig. 1*b*). In the double-labeled cells, the BrdU staining was strong and equally distributed throughout the nucleus (Fig. 1*c*–*n*). Most BrdU-NeuN immunoreactive cells were localized within the damaged area, especially medially and dorsally. Also, in the seemingly unaffected medial striatum, there was increased density of double-labeled neurons (28.7 ± 12.2 cells per mm^3; $P < 0.05$, Mann–Whitney U-test) (Fig. 1*b*). We found no clearly BrdU-NeuN double-labeled cells in or around the infarcted area of the parietal cortex.

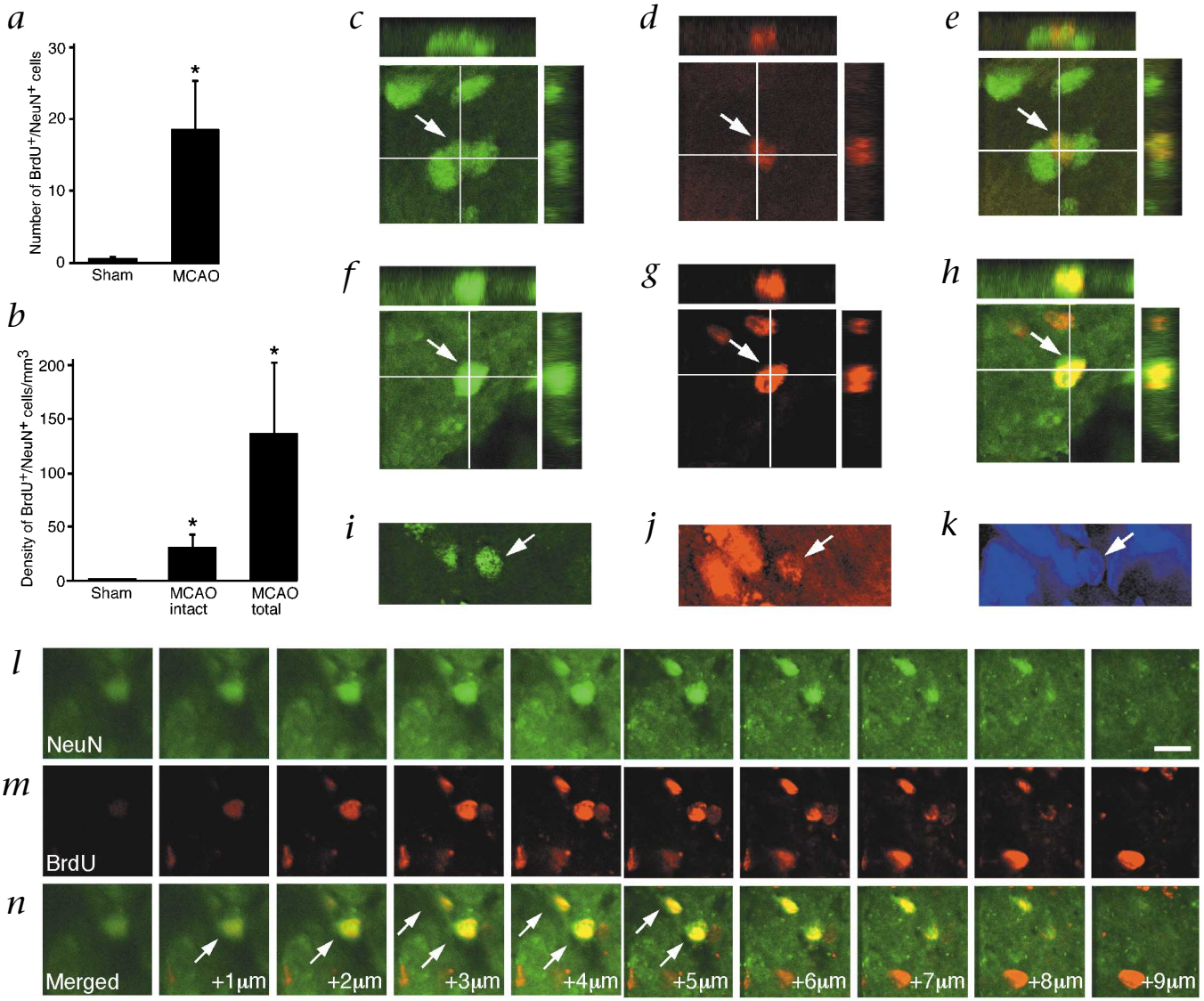

Fig. 1 Stroke-induced neurogenesis in the adult striatum. ***a*** and ***b***, Number (*a*) and density (*b*) of cells double-labeled with BrdU and NeuN in the striatum ipsilateral to sham surgery or 2 h of MCAO followed by BrdU injections at days 4–6 and 4 weeks of survival, as quantified with confocal microscopy in six 20-μm brain sections. Data are means ± s.e.m.; *, $P < 0.005$ (*a*); *, $P < 0.0005$ (*b*) compared with sham surgery, Mann–Whitney U-test. $n = 10$ and 9 for sham and MCAO, respectively. Densities in *b* are shown separately for parts of the striatum undamaged by the ischemia (MCAO intact) and for all striatal tissue (MCAO total). ***c–h***, Confocal 3D reconstruction of neurons from the intact (*c–e*) and lesioned (*f–h*) parts of the striatum ipsilateral to MCAO showing NeuN (*c* and *f*) or BrdU (*d* and *g*) immunoreactivity separately or as a merged image (*e* and *h*). Reconstructed orthogonal images are presented as viewed in the *x–z* (top) and *y–z* (right) planes. ***i–k***, Examples of striatal cells immunoreactive for NeuN (*i*, green) and BrdU (*j*, red) and labeled with the nuclear stain DAPI (*k*, blue). ***l–n***, 10 consecutive 1-μm confocal images in *z*-dimension showing NeuN (*l*) or BrdU (*m*) immunoreactivity separately or as merged images (*n*). Arrows indicate double-labeled cells. Scale bar, 15 μm.

Stroke triggers proliferation and recruitment of neuroblasts

The new neurons could originate from either the SVZ or from progenitors residing in the striatal parenchyma. We first investigated whether the insult had increased cell proliferation in the SVZ. Animals were given BrdU injections twice daily for two weeks after stroke and were sacrificed one day thereafter. Both the area covered by the BrdU-labeled cells and their number in the SVZ were markedly increased on the ischemic as compared with the contralateral side (area, 64,400 ± 7,000 and 42,600 ± 3,000 μm², $P < 0.05$; cell number, 639 ± 111 and 289 ± 36 cells per section, $P < 0.01$, respectively; paired *t*-test, $n = 9$). In contrast, the side difference in sham-operated rats was only marginal (area, 47,200 ± 2,200 and 48,500 ± 2,500 μm², $P > 0.05$; cell number, 395 ± 15 and 342 ± 18 cells/section, $P < 0.05$, respectively; paired *t*-test, $n = 5$).

To confirm that BrdU incorporation following stroke was due to cell proliferation in the SVZ, we infused the antimitotic drug cytosine-β-D-arabinofuranoside (Ara-C)[14] during the 12-day period after stroke and injected BrdU in parallel. Ara-C treatment inhibits cell proliferation in the mouse SVZ (ref. 14). The MCAO gave rise to an increase in SVZ size and BrdU⁺ cell numbers in saline-treated animals at one day after the last BrdU injection, but these values were markedly reduced by Ara-C treatment (area, 68,900 ± 6,500 and 30,300 ± 3,100 μm²; cell number, 1,027 ± 166 and 174 ± 36 cells per section for saline and Ara-C treated animals, respectively; $n = 5$ and 8; $P < 0.0001$ for both comparisons; unpaired *t*-test) (Fig. 2*a*).

To assess the role of cell proliferation in the generation of new striatal neurons, we stained for a marker of migrating neuroblasts, doublecortin (Dcx). In the adult brain, Dcx is expressed in the SVZ and rostral migratory stream but only single cells are detected in the striatum[15]. We found a similar pattern of expression on the side contralateral to stroke in the saline-treated animals, whereas Dcx-labeled cells were abundant on the ipsilateral side (Fig. 2*b* and *c*). After Ara-C treatment, the number of BrdU-Dcx double-labeled cells was markedly reduced in the ischemic striatum ($P < 0.005$, unpaired *t*-test) (Fig. 2*b–l*), whereas there remained numerous Dcx-stained, BrdU$^-$ cells ($P > 0.05$ (see Fig. 2*b*, unpaired *t*-test) (Fig. 2*b* and *j–l*). This finding indicates that most but not all of the new striatal neurons had been generated through stroke-induced cell proliferation in the SVZ or striatal parenchyma.

Stroke-generated neurons migrate from SVZ to damaged area

In the animals which were given BrdU injections for 14 days after the insult and killed directly thereafter, large numbers of Dcx-immunoreactive neurons appeared to migrate from the SVZ laterally and ventrally into the damaged area in the ischemic striatum (Fig. 3*b*). In contrast, both contralateral to the insult and in the rats subjected to sham procedure, Dcx immunoreactivity was confined to the SVZ and single striatal cells (Fig. 3*a* and *c*). No Dcx-immunoreactive cells were observed in or around the infarcted area of the parietal cortex.

The stroke-generated Dcx$^+$ cells showed morphologies characteristic of both migrating (elongated and leading processes) (Fig. 3*d–f*) and non-migrating cells (more symmetric with several processes in different directions) (Fig. 3*g–i*). The elongated Dcx$^+$ cells sometimes formed aggregates resembling chains. Confocal microscopy showed that 62% of the Dcx-immunoreactive neurons were also labeled with BrdU. Unlike the BrdU-NeuN-double-labeled cells, which were preferentially located in the damaged area at 5 weeks, the BrdU-Dcx-stained cells detected at 2 weeks were distributed along a gradient from the SVZ into the striatal parenchyma. Typically, more than half of these cells were located up to 0.5 mm laterally from the SVZ, and their density then gradually tapered off. Scattered cells could be observed up to approximately 2 mm from the SVZ. Most cells with migrating morphology had their leading processes directed away from the SVZ.

Because the results of the Ara-C treatment suggested that about half of the Dcx$^+$BrdU$^-$ neurons were generated after the stroke, the BrdU labeling probably underestimates the magnitude of striatal neurogenesis. Also, in brain areas normally sustaining adult neurogenesis, that is, DG and olfactory bulb, we found cells labeled only with Dcx along with a high number of Dcx$^+$ cells colabeled with BrdU (Fig. 3*j–m*). We therefore used Dcx as the main marker of newly formed striatal neurons for the further characterization of their phenotype during early development.

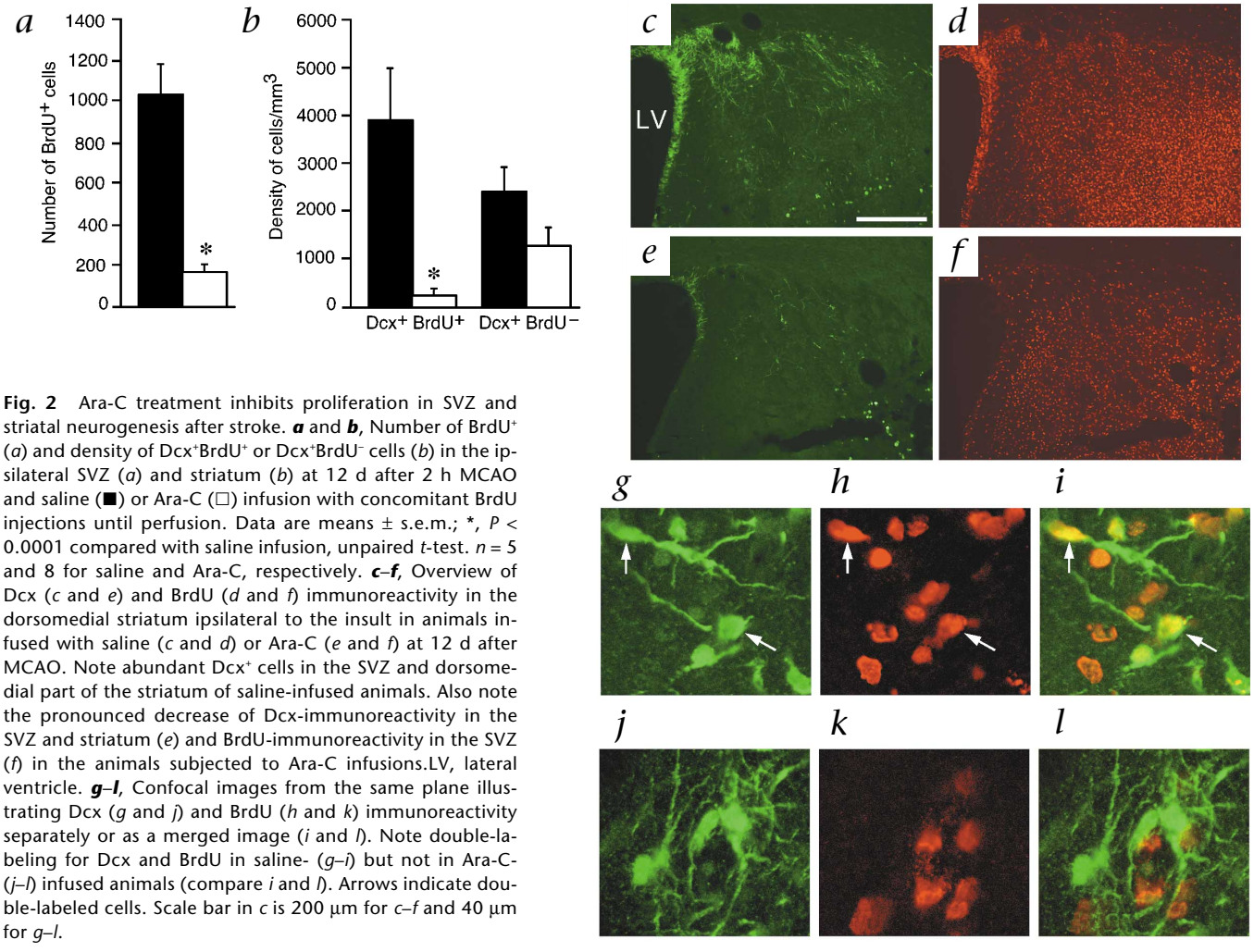

Fig. 2 Ara-C treatment inhibits proliferation in SVZ and striatal neurogenesis after stroke. ***a*** and ***b***, Number of BrdU$^+$ (*a*) and density of Dcx$^+$BrdU$^+$ or Dcx$^+$BrdU$^-$ cells (*b*) in the ipsilateral SVZ (*a*) and striatum (*b*) at 12 d after 2 h MCAO and saline (■) or Ara-C (□) infusion with concomitant BrdU injections until perfusion. Data are means ± s.e.m.; *, $P < 0.0001$ compared with saline infusion, unpaired *t*-test. $n = 5$ and 8 for saline and Ara-C, respectively. ***c–f***, Overview of Dcx (*c* and *e*) and BrdU (*d* and *f*) immunoreactivity in the dorsomedial striatum ipsilateral to the insult in animals infused with saline (*c* and *d*) or Ara-C (*e* and *f*) at 12 d after MCAO. Note abundant Dcx$^+$ cells in the SVZ and dorsomedial part of the striatum of saline-infused animals. Also note the pronounced decrease of Dcx-immunoreactivity in the SVZ and striatum (*e*) and BrdU-immunoreactivity in the SVZ (*f*) in the animals subjected to Ara-C infusions.LV, lateral ventricle. ***g–l***, Confocal images from the same plane illustrating Dcx (*g* and *j*) and BrdU (*h* and *k*) immunoreactivity separately or as a merged image (*i* and *l*). Note double-labeling for Dcx and BrdU in saline- (*g–i*) but not in Ara-C- (*j–l*) infused animals (compare *i* and *l*). Arrows indicate double-labeled cells. Scale bar in *c* is 200 µm for *c–f* and 40 µm for *g–l*.

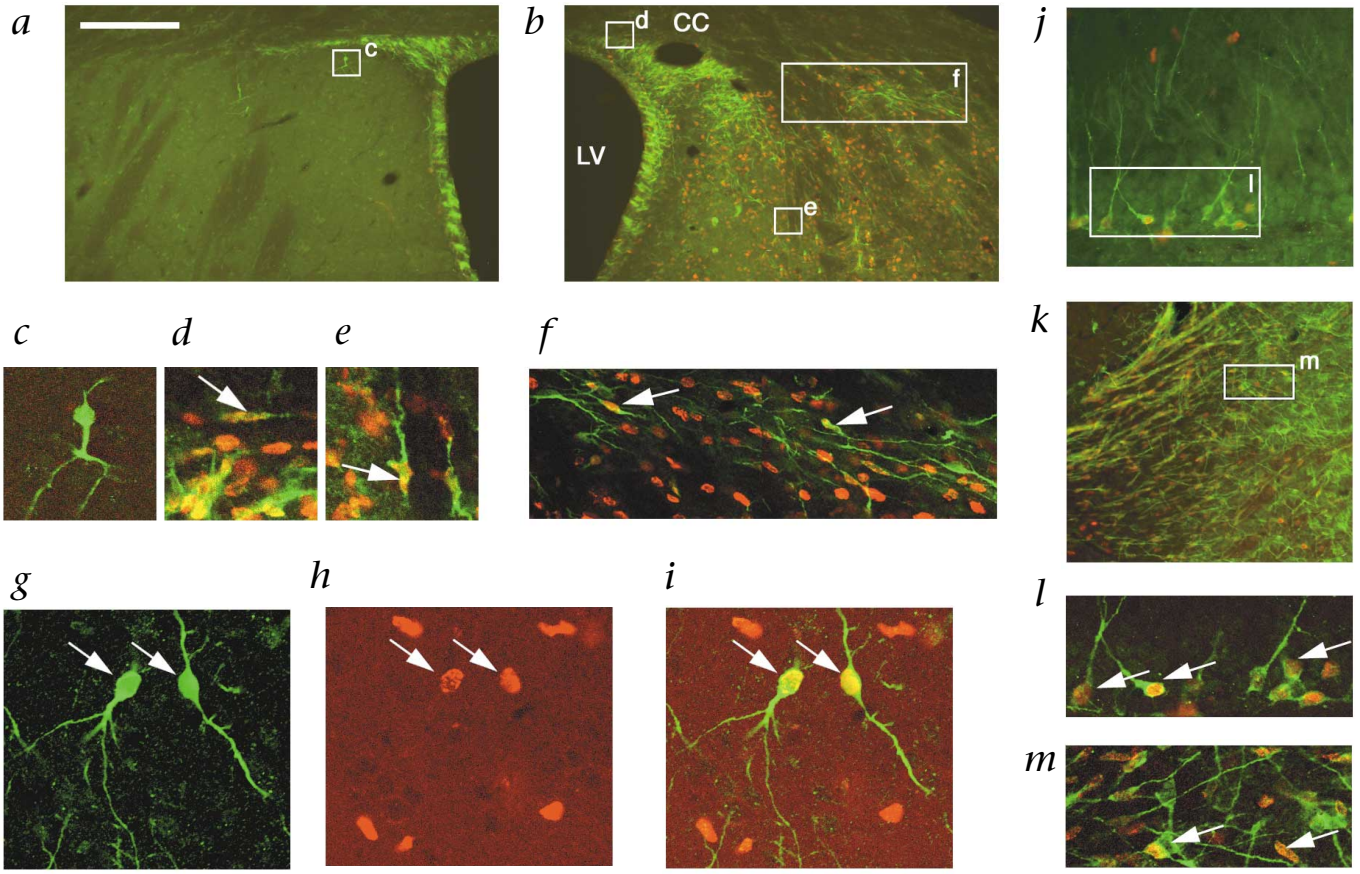

Fig. 3 Stroke-generated cells migrate from the subventricular zone into the ischemic lesion. ***a*** and ***b***, Overview of Dcx (green) and BrdU (red) immunoreactivity in the dorsomedial striatum contralateral (*a*) and ipsilateral (*b*) to the insult at 2 wk after MCAO. On the contralateral side, Dcx immunoreactivity is restricted to the SVZ and isolated cells in the striatum (*a*), whereas abundant Dcx$^+$ cells are present in the ipsilateral striatum (*b*), distributed in a density gradient from the SVZ, bordered dorsally by the corpus callosum (CC) and medially by the lateral ventricle (LV). ***c–f***, Confocal microscopy images showing the boxed areas in *a* and *b*. *c*, A Dcx$^+$BrdU$^-$ cell with the morphology of a mature neuron located in the striatum contralateral to MCAO. *d*, Densely clustered Dcx$^+$ cells in the SVZ, showing extensive colocalization with BrdU immunoreactivity. A migrating Dcx-BrdU double-labeled cell can be seen in the CC dorsal to the SVZ (arrow). *e*, A Dcx$^+$ cell with the morphology of a migrating neuroblast double-labeled with BrdU. *f*, Multiple Dcx-labeled cells with migratory or mature morphologies. Some of the cells are double-labeled with BrdU (arrows). ***g–i***, Confocal images of two neurons with mature morphology from the striatum ipsilateral to MCAO showing Dcx (*g*) or BrdU (*h*) immunoreactivity separately or as a merged image (*i*). ***j–m***, Overviews (*j* and *k*) and confocal images (*l* and *m*) showing boxed areas in *j* and *k*, of Dcx and BrdU immunoreactivity in the dentate gyrus (*j* and *l*) and olfactory bulb (*k* and *m*) ipsilateral to sham surgery. There is extensive, but not complete, colocalization of Dcx and BrdU immunoreactivity. Scale bar in *a* is 200 μm for *a*, *b* and *k*, 40 μm for *c–e*, *l* and *m*, 50 μm *g–l* and 60 μm for *j*.

New cells express markers of striatal medium spiny neurons

In order to determine whether the new neurons developed striatal-specific characteristics, we first analyzed their expression of the transcription factor Meis2 at 2 weeks after stroke. Meis2 is normally expressed in proliferating precursors that differentiate into striatal neurons, but is also expressed in the adult striatum where the expression closely resembles that of the marker for medium-sized spiny neurons, DARPP-32 (ref. 16). Confocal microscopy showed that virtually all Dcx$^+$ cells (96%) were Meis2$^+$ (Fig. 4*a–c*). The expression of Pbx proteins, which are colocalized with Meis2 in developing striatal neurons[16], coincided with that of Meis2, and almost all Dcx$^+$ cells (94%) (Fig. 4*d–f*) were also labeled with Pbx. We found similarly high coexpression of Dcx and Hu (93%) (Fig. 4*g–i*), an early neuronal marker[17,18]. There was also extensive colocalization of BrdU with Meis2, Pbx or Hu in the SVZ and striatum (Fig. 4*j–r*). In addition, Meis2 was expressed in Dcx$^-$ and BrdU$^-$ striatal neurons on the lesioned and non-lesioned side. However, the Meis2 immunoreactivity was stronger in the cells colabeled with BrdU or Dcx as compared with the other striatal neurons. This finding is consistent with previous observations that Meis2 expression is higher in developing than in mature striatal neurons[19]. We did not observe a single Dcx-labeled cell that coexpressed markers of glial precursors or mature glia, that is as NG-2, vimentin and glial fibrillary acidic protein (GFAP).

At two weeks after the stroke, 20% of Dcx$^+$ striatal cells also expressed NeuN, indicating that some of the young cells had already differentiated into mature neurons. This was substantiated by the finding of cells double-labeled with BrdU and NeuN in the same brains (Table 1). We then allowed an additional group of rats, subjected to the same regimen of BrdU injections, to survive for 4 weeks following the last injection. The number and density of BrdU-NeuN double-labeled cells was 4.9- and 9.7-fold higher, respectively, in the ischemic striatum of these animals as compared with those that had been sacrificed directly following the last BrdU injection ($P <$ 0.005 for both number and density, Mann–Whitney U-test,

n = 9 and 6 for short-term and long-term survival groups, respectively) (Table 1). Thus, longer survival time allowed for more of the proliferated cells to differentiate into mature neurons.

To further explore whether the new neurons adopted the phenotype of medium-sized spiny neurons, the dominant striatal neuron type, we used an antibody to a selective marker for these neurons, DARPP-32 (refs. 20,21) (Fig. 5). At 5 weeks following the insult, using BrdU-injections during days 4–6, the density of DARPP-32-BrdU$^+$ cells was 56.9 ± 22.6 cells/mm^3, which was 42% of the density of BrdU-NeuN double-labeled cells. There was a good correlation between the densities of NeuN and DARPP-32$^+$ cells double-labeled with BrdU (r = 0.68, P = 0.053), indicating that the proportion of newly formed neurons that expressed the marker of medium-sized spiny neurons was similar in the different animals (Fig. 5*a*). After 2 weeks of daily BrdU injections and 4 weeks of survival, the density of BrdU-DARPP-32 double-labeled cells was 312.6 ± 109.4 cells/mm^3 (Table 1).

Discussion

Cell-replacement strategies to restore function in neurodegenerative disorders have been based on intracerebral transplantation of primary fetal cells, progenitor cells predifferentiated *in vitro* or stem cells[22]. These studies have shown that neuronal replacement and partial reconstruction of neuronal circuitry can be achieved in the adult brain by cell transplantation. Here we provide the first evidence that the adult brain can use neuronal replacement from endogenous precursors to repair itself after stroke.

Following an ischemic insult which gave rise to severe damage in the striatum, new neurons were generated through proliferation of precursor cells in the SVZ and possibly also in the striatal parenchyma. It is highly unlikely that Dcx expression had been induced in adult neurons by the ischemic damage, or that the BrdU-labeled cells were adult neurons undergoing apoptosis or DNA repair. Accordingly, we found no Dcx-immunoreactive or BrdU-NeuN double-labeled cells in the parietal cortex, which also showed extensive ischemic damage. However, there were increased numbers of BrdU-Dcx double-labeled neurons in the DG, which is not damaged after this insult and where stroke-induced neurogenesis occurs[6]. BrdU colocalized with markers of both developing and mature striatal neurons, and colocalization with NeuN, a marker of mature neurons, increased several-fold over a four-week period after two weeks of BrdU injections. The BrdU immunoreactivity did not have a punctuate appearance but was

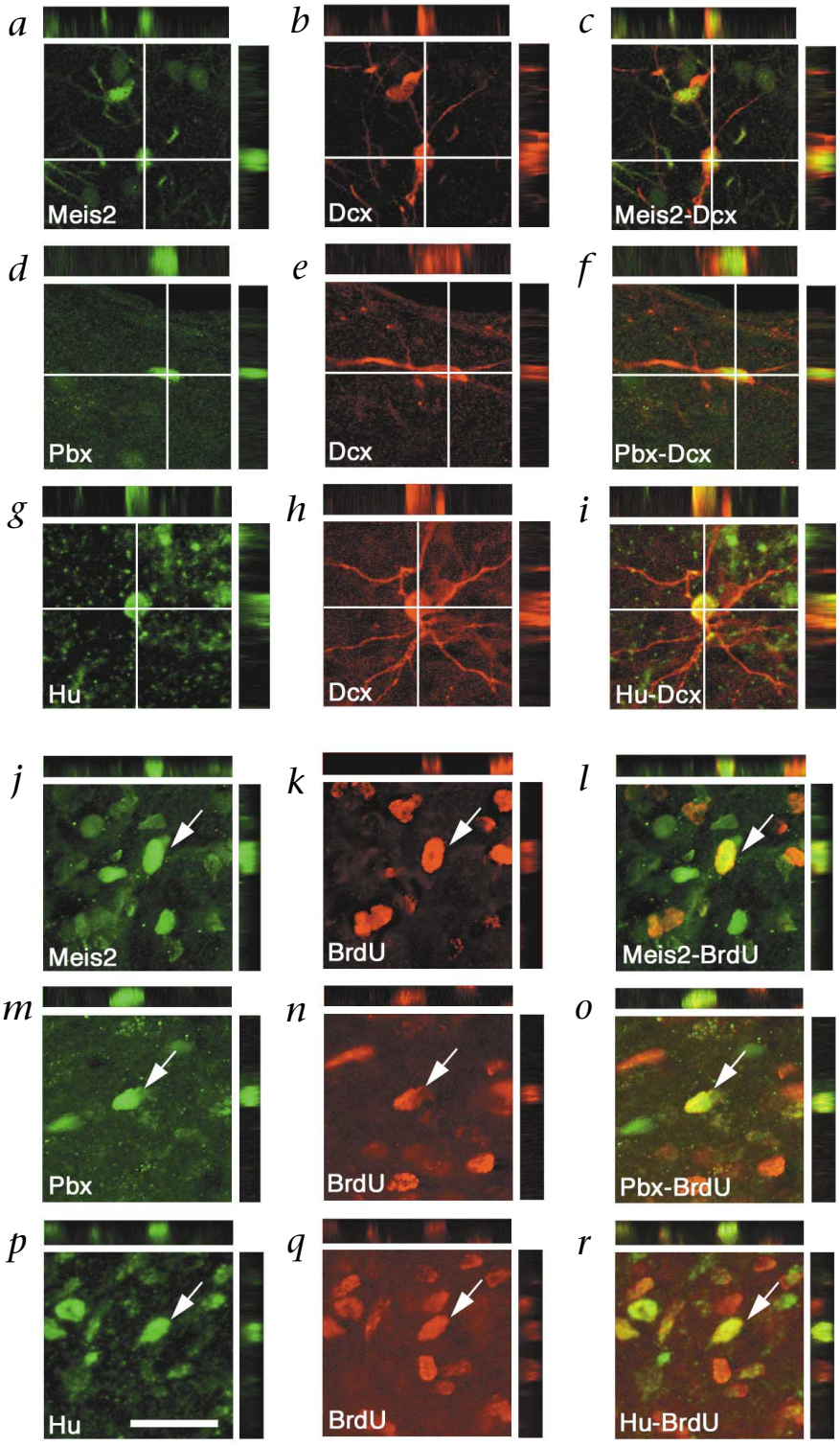

Fig. 4 Stroke-generated cells express markers of developing striatal neurons. Confocal images of immunohistochemically stained cells at 2 weeks following MCAO. ***a*–*i***, Dcx (*b*, *e*, and *h*), Meis2 (*a*), and Pbx (*d*) or Hu (*g*) immunoreactivity separately or as merged images (*c*, *f*, and *i*). ***j*– *r***, BrdU (*k*, *n*, and *q*) and Meis2 (*j*), Pbx (*m*) or Hu (*p*) immunoreactivity separately or as merged images (*l*, *o*, and *r*). Orthogonal reconstructions of double-labeled cells are presented as viewed in the *x*–*z* (top) and *y*–*z* (right) planes. Scale bar in *p* is 50 μm for *a*–*i* and 25 μm for *j*–*r*.

distributed throughout the nucleus. Furthermore, a similar ischemic insult caused no detectable DNA damage in the SVZ (ref. 7). We also observed that the mitosis inhibitor Ara-C gave rise to a marked reduction (93%) of the number of BrdU-Dcx double-labeled striatal cells as compared with vehicle-injected animals, without any effect on the extent of striatal damage. In contrast, the total number of Dcx^+ cells was only decreased by 75%. These findings confirm that cell proliferation has a major role for neurogenesis in the striatum following stroke. However, the fact that 25% of the new striatal Dcx^+ neurons (virtually all $BrdU^-$) remained despite Ara-C treatment also indicates that neuroblasts that have undergone division before the insult are recruited to the damaged area.

Our findings indicate that ischemic neuronal death transmits signals to the new neurons to migrate into the damaged area of the striatum. A flow of new neurons with migratory morphologies could be traced back to the SVZ, i.e., over a distance of up to 2 mm. These neurons sometimes formed aggregates, suggesting that some of them may reach the damaged area using chain migration, similar to neuronal precursors in the rostral migratory stream[23,24]. The nature of the signaling molecules attracting the new neurons is unclear. Such signals could also explain why transplanted neuronal precursors and neuroepithelial stem cells migrate to a tumor[25] or ischemic lesion[26], respectively, in the contralateral hemisphere. It might also explain why stem cells grafted at the border of the striatal lesion following MCAO preferentially migrate into the damaged area (data not shown). The recent demonstration[27] of an astrocyte-derived migration-inducing activity, regulating the migration of SVZ neuronal precursors, suggests that astrocytes in the ischemic lesion[13] may have an important role.

There is no evidence for constitutive formation of new striatal-specific neurons in the normal adult striatum[28]. When the adult SVZ is transplanted into the adult striatum, the few cells that differentiate into neurons resemble olfactory-bulb interneurons[29]. However, new striatal neurons expressing markers of medium-sized spiny neurons can be formed when brain-derived neurotrophic factor (BDNF) is overexpressed in the ventricular zone using a viral vector[28]. We found that stroke generated large numbers of new cells in the striatum, which expressed not only general markers of developing (Dcx and Hu) and adult neurons (NeuN), but also markers of both developing (Meis2 and Pbx) and mature striatal medium-sized spiny neurons (DARPP-32). Thus, the new neurons differentiated into the phenotype of most of the neurons destroyed by the ischemic lesion. When new neocortical neurons were induced following apoptosis of a subset of neurons, other tissue architecture remained intact[10]. Following stroke, the new neurons migrate into a severely damaged area and local microenvironmental signals necessary for neuronal differentiation are likely to be inadequate. This raises the possibility that the neuroblasts reaching the damaged striatum are already committed to become medium-sized spiny neurons.

It is interesting, in view of the findings of Magavi *et al.*[10], that we detected no neurogenesis in the damaged cerebral cortex following stroke. The new neocortical neurons generated by selective photolytic lesion probably originated from both the SVZ and from local neural precursors[10]. The lack of cortical neurogenesis in our experiments could be caused by an unfavorable microenvironment for the local precursors. Also, the large ischemic lesion in the striatum may attract new neurons formed in the SVZ more efficiently as compared with a more distant cortical lesion.

At two weeks after stroke we observed about 6,300 Dcx^+ new neurons per mm^3 in the damaged striatum, showing that the neurogenic response is substantial. Based on comparisons between the density of BrdU-stained cells colabeled with a neuronal marker at 2 (Dcx) and 6 (NeuN) weeks post-ischemia (Table 1), we estimate that about 80% or more of the new neurons died during this time interval. We obtained no evidence that any of the Dcx-labeled cells observed at 2 weeks were destined to become glial cells. The major cell loss following stroke is comparable to that observed for SGZ cells, which have proliferated after status epilepticus[30]. This low survival of newly formed neurons most likely reflects an unfavorable environment with lack of trophic support and connections, and exposure to the detrimental actions of severely damaged tissue.

Stroke is one of the most common causes of death and disability in humans. Our results demonstrate that mechanisms for neuronal replacement from endogenous precursors following stroke operate in the adult brain: neuronal precursors proliferate in the SVZ and possibly also locally in the striatum, and the newly formed neurons migrate into the ischemic lesion and differentiate into the phenotype of the degenerated neurons. We estimate that the fraction of dead striatal neurons that has been replaced by the new neurons at 6 weeks after insult is small—only about 0.2%. It is yet unclear to what extent this number of neurons (about 1,600) can contribute to reconstruction of striatal neural circuitry and functional recovery after stroke. However, recent studies indicate that administration of BDNF into the lateral ventricle or to the SVZ can stimulate neurogenesis in the striatum[28,31]. Moreover, we show that the initial generation of neuroblasts following stroke far exceeds the final number of surviving new neurons. Such data support the notion that the neurogenic response following stroke might be amplified. If the new neurons also are functional, completely novel treatment strategies might be developed for patients affected by this disorder.

Table 1 Neurogenesis in the ischemic striatum

Time after stroke	BrdU injections	Number of labeled cells per mm3			
		$BrdU^+$ $NeuN^+$	$BrdU^+$ $DARPP\text{-}32^+$	Dcx+	$BrdU^+$ Dcx^+
2 wk	Days 1–12 or 1-14	77.6 ± 38.4 (*n* = 9)		6,312 ± 1,529 (*n* = 5)	3,898 ± 1,040 (*n* = 5)
5 wk	Days 4–6	136.7 ± 66.7 (*n* = 9)	56.9 ± 22.6 (*n* = 9)		
6 wk	Days 1–14	749.8 ± 213.5 (*n* = 6)	312.6 ± 109.4 (*n* = 6)		

Neurogenesis recorded at different time-points following stroke expressed as density of cells labeled with various neuronal markers. Values are means ± s.e.m. BrdU (50 mg/kg i.p.) was given twice daily.

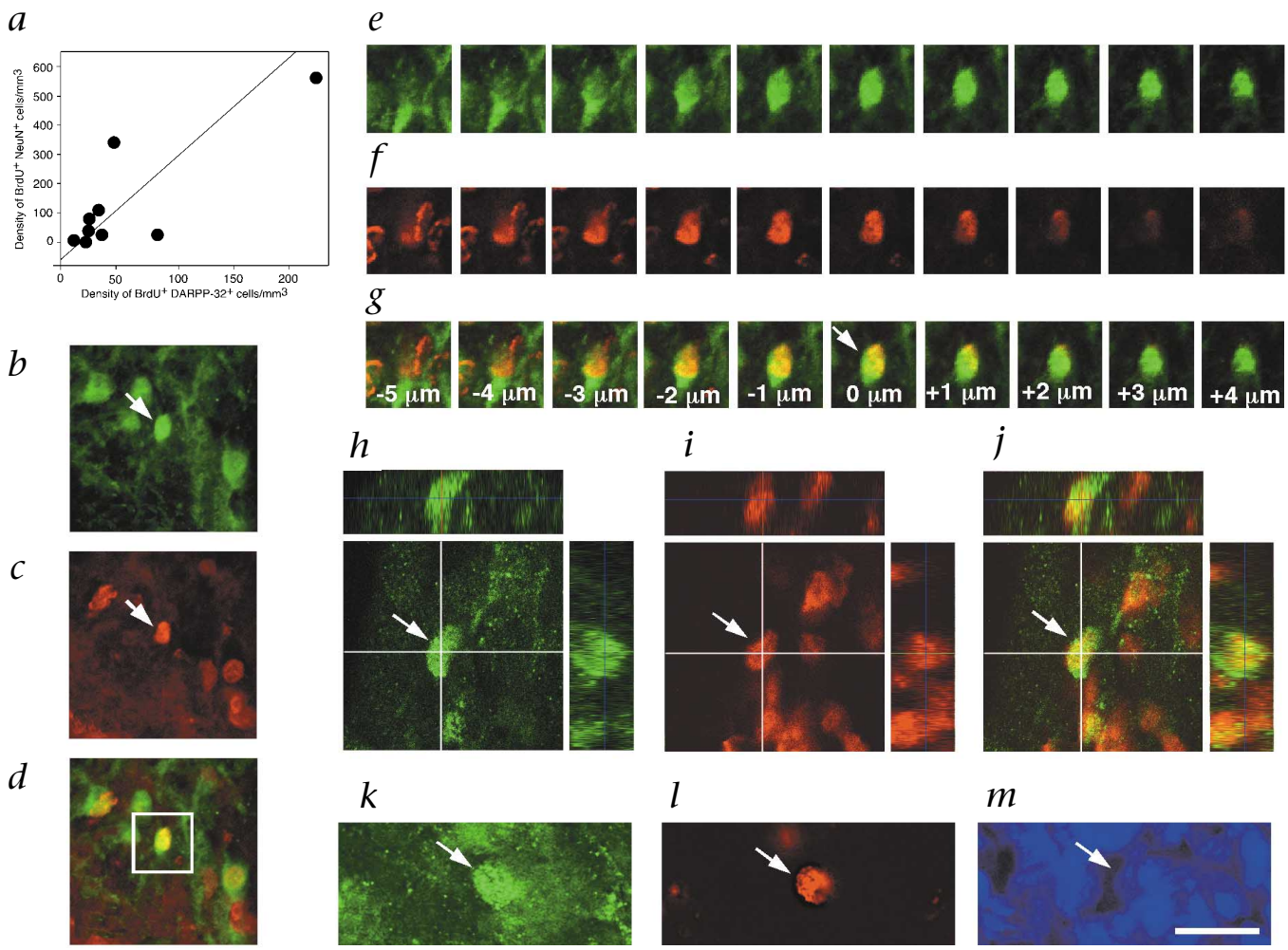

Fig. 5 Stroke-generated cells express markers of mature striatal medium-sized spiny neurons. ***a***, Relationship between the density of BrdU-NeuN and BrdU-DARPP-32 double-labeled cells in the striatum ipsilateral to MCAO. Each animal is plotted individually and the line shows the linear regression for the relationship between $BrdU^+DARPP\text{-}32^+$ and $BrdU^+NeuN^+$ cell density (Spearman's $r = 0.68$, $P = 0.053$). ***b–j***, Confocal images showing double-labeling for DARPP-32 (green) and BrdU (red). Arrows indicate double-labeled cells. *b–d*, Images from the same confocal plane showing DARPP-32 (*b*) or BrdU (*c*) immunoreactivity separately or as merged image (*d*). *e–g*, 10 consecutive optical sections of a *z*-series through the same cell as in *b–d* (box in *d*) showing DARPP-32 (*e*) or BrdU (*f*) immunoreactivity separately or as merged images (*g*). Values indicate the relative distance in the *z*-direction from the confocal plane in *b–d* (0 µm). *h–j*, Confocal 3D reconstruction of a neuron from the lesioned part of the striatum showing DARPP-32 (*h*) or BrdU (*i*) immunoreactivity separately or as a merged image (*j*). Reconstructed orthogonal images are presented as viewed in the *x–z* (top) and *y–z* (right) planes. ***k–m***, Example of a striatal cell immunoreactive for DARPP-32 (*k*, green) and BrdU (*l*, red) and stained with DAPI (*m*, blue). Scale bar in *m* is 40 µm for *b–d*, 30 µm for *e–j* and 20 µm *k–m*.

Methods

Induction of stroke. Under halothane anesthesia, the middle cerebral artery of artificially ventilated male Wistar rats was occluded with a nylon monofilament inserted through the common carotid artery[32–34]. After 2 h, the filament was withdrawn. For sham surgery, the filament was advanced only a few mm inside the internal carotid artery. Body temperature, arterial blood pressure, pO_2, pCO_2 and pH were monitored during surgery and kept within a predetermined physiological range.

BrdU labeling and anti-mitotic treatment. Intraperitoneal injections of BrdU (50 mg/kg, Sigma-Aldrich, St. Louis, Missouri) were given twice daily during days 4–6 or 1–14 after MCAO or sham surgery. In one experiment, rats were implanted just before MCAO with mini-osmotic pumps (model 2002, flow rate 0.5 µl/h; Alzet, Palo Alto, California,) continuously infusing either Ara-C (2% (Sigma-Aldrich) in 0.9% saline) or saline on the surface of the brain[14]. Infusion was continued for 12 d and BrdU injections were given concomitantly. Animals were killed at 1 d or 4 wk after the last BrdU injection.

Immunohistochemistry. After transcardial perfusion with 4% ice-cold phosphate-buffered paraformaldehyde (PFA), brains were post-fixed in 4% PFA and sectioned in the coronal plane at 20, 30 or 40 µm on powdered dry ice. The sections were then double stained for BrdU or Dcx and various neuronal markers. Free-floating sections were denatured by incubation in 1 M hydrochloric acid at 65 °C for 30 min before BrdU staining. Sections were then incubated for 36 h with rat antibody against BrdU (1:100, Harlan Sera-Lab, Loughborough, UK) and rabbit anti-Dcx antibody (1:250, provided by J.G. Gleeson and C.A. Walsh) or either of these in combination with one of the following antibodies: mouse anti-NeuN (1:100, Chemicon, Temecula, California), mouse anti-Hu (1:1000, provided by S.A. Goldman), rabbit anti-Meis2 (1:1000, provided by A.M. Buchberg), rabbit anti-Pbx 1/2/3 (1:400, Santa Cruz Biotechnology Inc, Santa Cruz, California), mouse anti-DARPP-32 (1:20000, provided by P. Greengard), mouse anti-GFAP (1:1000, Sigma-Aldrich), mouse anti-vimentin (1:25, DAKO, Glostrup, Denmark) or rabbit anti-NG2 (1:100, Chemicon) with appropriate normal sera. When two antibodies originated from the same species, double labeling was performed as sequential stainings, with controlled cross-reactivity. Sections were rinsed and

incubated for 2 h with Cy3-conjugated (Jackson ImmunoResearch, West Grove, Pennsylvania) or biotinylated (Vector, Burlingame, California) secondary antibodies (1:200). After rinsing, sections were incubated for 2 h with Alexa 488-conjugated streptavidin (1:200, Molecular Probes, Eugene, Oregon), mounted on super-plus slides and cover-slipped. When staining for Hu, the avidin step was preceded by tyramide amplification procedure (TSA biotin system, NEN Life Science Products, Boston, MA). For counter-staining with DAPI (Sigma-Aldrich), hydrochloric acid treatment was performed at 37 °C.

Microscopical analysis. Cells double-labeled with BrdU and NeuN or DARPP-32 were counted with an epifluorescence microscope using ×40 objective. In animals given BrdU during days 4–6 and killed 4 wk later, striatum was screened in 3 pairs of 20-μm coronal sections (BrdU-NeuN) or 3 single 40-μm sections (BrdU-DARPP-32) at +0.92, +0.56 and +0.20 mm from bregma. Cells were equally distributed at all levels, and were therefore counted in a single 30-μm section (+0.50 from bregma) per animal in other experiments. The accuracy of counting of double-labeled cells using epifluorescence microscopy was determined by analysis of 84–86 (MCAO-animals) or all (sham animals) systematically sampled candidate cells per staining with a confocal laser scanning microscope (BioRad Microscience, Hemel Hempstead, UK). All cell numbers and densities were adjusted according to the percentage of this confocal validation. Cells were considered double-labeled if colabeling with relevant morphology was seen throughout the extent of the nucleus for nuclear markers, or if a cytoplasmic marker surrounded a nuclear marker, when viewed in *x–y* cross section, as well as in *x–z* and *y–z* cross-sections produced by orthogonal reconstructions from *z*-series (*z*-step, 1 μm) taken with ×40 objective. Dcx-labeled cells were counted in three 30-μm sections from rostrocaudal levels as above. Double labeling with BrdU or phenotypic markers was determined by random sampling of 100 or more Dcx^+ cells per marker for analysis by confocal microscopy, and the density of double-labeled cells was calculated from individual values of Dcx^+ cell density and proportion of double labeling. $BrdU^+$ cells in the SVZ were counted in one 30-μm section per animal (+0.50 mm from bregma) using the fractionator method on stereological equipment. Areas were measured using stereological equipment in sections double-stained for NeuN and BrdU.

Statistical analysis. Values are means ± s.e.m. Numbers or densities of newly formed cells were assessed with unpaired *t*-test or Mann–Whitney U-test, and side differences in cell numbers or areas with paired *t*-test. Spearman's correlation coefficient was used to assess correlation between cell densities.

Acknowledgments

This work was supported by the Swedish Research Council, The Söderberg Foundation, Kock, Crafoord, and Elsa and Thorsten Segerfalk Foundations, the Swedish Stroke Foundation and the Swedish Association of Neurologically Disabled.

Competing interests statement

The authors declare that they have no competing financial interests.

RECEIVED 26 NOVEMBER 2001; ACCEPTED 16 JULY 2002

1. Gage, F.H. Mammalian neural stem cells. *Science* **287**, 1433–1438 (2000).
2. Reynolds, B.A. & Weiss, S. Generation of neurons and astrocytes from isolated cells of the adult mammalian central nervous system. *Science* **255**, 1707–1017 (1992).
3. Parent, J.M. *et al.* Dentate granule cell neurogenesis is increased by seizures and contributes to aberrant network reorganization in the adult rat hippocampus. *J. Neurosci.* **17**, 3727–3738 (1997).
4. Bengzon, J. *et al.* Apoptosis and proliferation of dentate gyrus neurons after single and intermittent limbic seizures. *Proc. Natl. Acad. Sci. USA* **94**, 10432–10437 (1997).
5. Liu, J., Solway, K., Messing, R.O. & Sharp, F.R. Increased neurogenesis in the dentate gyrus after transient global ischemia in gerbils. *J. Neurosci.* **18**, 7768–7778 (1998).
6. Arvidsson, A., Kokaia, Z. & Lindvall, O. *N*-methyl-D-aspartate receptor-mediated increase of neurogenesis in adult rat dentate gyrus following stroke. *Eur. J. Neurosci.* **14**, 10–18 (2001).
7. Jin, K. *et al.* Neurogenesis in dentate subgranular zone and rostral subventricular zone after focal cerebral ischemia in the rat. *Proc. Natl. Acad. Sci. USA* **98**, 4710–4715 (2001).
8. Zhang, R.L., Zhang, Z.G., Zhang, L. & Chopp, M. Proliferation and differentiation of progenitor cells in the cortex and the subventricular zone in the adult rat after focal cerebral ischemia. *Neuroscience* **105**, 33–41 (2001).
9. Gu, W., Brännström, T. & Wester, P. Cortical neurogenesis in adult rats after reversible photothrombotic stroke. *J. Cereb. Blood Flow Metab.* **20**, 1166–1173 (2000).
10. Magavi, S.S., Leavitt, B.R. & Macklis, J.D. Induction of neurogenesis in the neocortex of adult mice. *Nature* **405**, 951–955 (2000).
11. Heimer, L., Zahm, D.S. & Alheid, G.F. Basal ganglia. in *The Rat Nervous System* (ed. Paxinos, G.) 579–628 (Academic, San Diego, 1995).
12. Davies, C.A., Loddick, S.A., Stroemer, R.P., Hunt, J. & Rothwell, N.J. An integrated analysis of the progression of cell responses induced by permanent focal middle cerebral artery occlusion in the rat. *Exp. Neurol.* **154**, 199–212 (1998).
13. Stoll, G., Jander, S. & Schroeter, M. Inflammation and glial responses in ischemic brain lesions. *Prog. Neurobiol.* **56**, 149–171 (1998).
14. Doetsch, F., Garcia-Verdugo, J.M. & Alvarez-Buylla, A. Regeneration of a germinal layer in the adult mammalian brain. *Proc. Natl. Acad. Sci. USA* **96**, 11619–11624 (1999).
15. Nacher, J., Crespo, C. & McEwen, B.S. Doublecortin expression in the adult rat telencephalon. *Eur. J. Neurosci.* **14**, 629–644 (2001).
16. Toresson, H., Parmar, M. & Campbell, K. Expression of Meis and Pbx genes and their protein products in the developing telencephalon: implications for regional differentiation. *Mech. Dev.* **94**, 183–187 (2000).
17. Marusich, M.F., Furneaux, H.M., Henion, P.D. & Weston, J.A. Hu neuronal proteins are expressed in proliferating neurogenic cells. *J. Neurobiol.* **25**, 143–155 (1994).
18. Barami, K., Iversen, K., Furneaux, H. & Goldman, S.A. Hu protein as an early marker of neuronal phenotypic differentiation by subependymal zone cells of the adult songbird forebrain. *J. Neurobiol.* **28**, 82–101 (1995).
19. Toresson, H., Mata de Urquiza, A., Fagerstrom, C., Perlmann, T. & Campbell, K. Retinoids are produced by glia in the lateral ganglionic eminence and regulate striatal neuron differentiation. *Development* **126**, 1317–1326 (1999).
20. Ouimet, C.C., Miller, P.E., Hemmings, H.C. Jr, Walaas, S.I. & Greengard, P. DARPP-32, a dopamine- and adenosine 3′:5′-monophosphate-regulated phosphoprotein enriched in dopamine-innervated brain regions. III. Immunocytochemical localization. *J. Neurosci.* **4**, 111–124 (1984).
21. Ouimet, C.C., Langley-Gullion, K.C. & Greengard, P. Quantitative immunocytochemistry of DARPP-32-expressing neurons in the rat caudatoputamen. *Brain Res.* **808**, 8–12 (1998).
22. Björklund, A. & Lindvall, O. Cell replacement therapies for central nervous system disorders. *Nature Neurosci.* **3**, 537–544 (2000).
23. Lois, C., Garcia-Verdugo, J.M. & Alvarez-Buylla, A. Chain migration of neuronal precursors. *Science* **271**, 978–981 (1996).
24. Wichterle, H., Garcia-Verdugo, J.M. & Alvarez-Buylla, A. Direct evidence for homotypic, glia-independent neuronal migration. *Neuron* **18**, 779–791 (1997).
25. Aboody, K.S. *et al.* Neural stem cells display extensive tropism for pathology in adult brain: evidence from intracranial gliomas. *Proc. Natl. Acad. Sci. USA* **97**, 12846–12851 (2000).
26. Veizovic, T., Beech, J.S., Stroemer, R.P., Watson, W.P. & Hodges, H. Resolution of stroke deficits following contralateral grafts of conditionally immortal neuroepithelial stem cells. *Stroke* **32**, 1012–1019 (2001).
27. Mason, H.A., Ito, S. & Corfas, G. Extracellular signals that regulate the tangential migration of olfactory bulb neuronal precursors: Inducers, inhibitors, and repellents. *J. Neurosci.* **21**, 7654–7663 (2001).
28. Benraiss, A., Chmielnicki, E., Lerner, K., Roh, D. & Goldman, S.A. Adenoviral brain-derived neurotrophic factor induces both neostriatal and olfactory neuronal recruitment from endogenous progenitor cells in the adult forebrain. *J. Neurosci.* **21**, 6718–6731 (2001).
29. Herrera, D.G., Garcia-Verdugo, J.M. & Alvarez-Buylla, A. Adult-derived neural precursors transplanted into multiple regions in the adult brain. *Ann. Neurol.* **46**, 867–877 (1999).
30. Ekdahl, C.T., Mohapel, P., Elmér, E. & Lindvall, O. Caspase inhibitors increase short-term survival of progenitor-cell progeny in the adult rat dentate gyrus following status epilepticus. *Eur. J. Neurosci.* **14**, 937–945 (2001).
31. Pencea, V., Bingaman, K.D., Wiegand, S.J. & Luskin, M.B. Infusion of brain-derived neurotrophic factor into the lateral ventricle of the adult rat leads to new neurons in the parenchyma of the striatum, septum, thalamus, and hypothalamus. *J. Neurosci.* **21**, 6706–6717 (2001).
32. Koizumi, J., Yoshida, Y., Nakazawa, T. & Ooneda, G. Experimental studies of ischemic brain edema. 1. A new experimental model of cerebral embolism in rats in which recirculation can be introduced in the ischemic area. *Jpn. J. Stroke.* **8**, 1–8 (1986).
33. Zhao, Q., Memezawa, H., Smith, M.L. & Siesjö, B.K. Hyperthermia complicates middle cerebral artery occlusion induced by an intraluminal filament. *Brain Res.* **649**, 253–259 (1994).
34. Kokaia, Z. *et al.* Regulation of brain-derived neurotrophic factor gene expression after transient middle cerebral artery occlusion with and without brain damage. *Exp. Neurol.* **136**, 73–88 (1995).